Appended aromatic moieties determine the Cytotoxicity of Neutral Cyclometalated Platinum(II) complexes derived from 2-(2-Pyridyl)benzimidazole

Journal:	*Inorganic Chemistry*
Manuscript ID	ic-2020-00219f.R1
Manuscript Type:	Article
Date Submitted by the Author:	02-Mar-2020
Complete List of Authors:	Vaquero, Mónica; University of Burgos, Chemistry Department Busto, Natalia; Universidad de Burgos, Quimica Fernández-Pampín, Natalia; Universidad de Burgos Espino, Gustavo; Universidad de Burgos, Química Garcia, Begona; Universidad de Burgos, Quimica

Appended aromatic moieties determine the Cytotoxicity of Neutral Cyclometalated Platinum(II) complexes derived from 2-(2-Pyridyl)benzimidazole

Mónica Vaquero,*‡ Natalia Busto,‡ Natalia Fernández-Pampín, Gustavo Espino, Begoña García.*

Departamento de Química, Facultad de Ciencias, Universidad de Burgos, Plaza Misael Bañuelos s/n, 09001, Burgos, Spain.

KEYWORDS. Cyclometalated Pt(II) complexes, Axial chirality, Pyridylbenzimidazole, DNA Binding, Cytotoxicity.

Supporting Information Placeholder

ABSTRACT: A new family of neutral chiral cyclometalated platinum(II) complexes with formula [Pt(κ^2-(**C^N**))Cl(κ^1-(**L**))], where (**C^N**) = 2-phenylpyridinate and (**L**) = 2-(2-Pyridyl)benzimidazole (**L1**) or (N-(CH_2)-**Ar**-(2-(2-Pyridyl)benzimidazole) ligands; (**Ar** = phenyl (**L2**), naphthyl (**L3**), pyrenyl (**L4**)), have been synthesized and completely characterized. The unexpected κ^1 coordination mode of the 2-(2-Pyridyl)benzimidazole-derived ligands has been confirmed by spectroscopic techniques and X-Ray diffraction. The aromatic moieties on the ligands in the new platinum(II) complexes have a remarkable influence on the cytotoxicity and in the binding mode to DNA. **[Pt-L1]-[Pt-L4]** complexes internalized more than cisplatin in the SW480 cancer cells even though only **[Pt-L1]** and **[Pt-L2]** display highest cytotoxicity. ^{1}H NMR and ^{31}P NMR pointed that **[Pt-L1]** and **[Pt-L2]** complexes bind covalently to *d*GMP, while the electrophoresis assays and CD experiments indicate that only **[Pt-L2]** is able to covalently interact with DNA, inducing the same conformational changes in the plasmid DNA as cisplatin. Although the complex **[Pt-L4]** intercalate into DNA, probably through the pyrenyl moiety, no biological activity is observed.

INTRODUCTION

Nowadays, cytotoxic platinum(II) complexes are the most effective anticancer drugs used in chemotherapy.[1–3] Since cisplatin was accidentally discover by Rosenberg in 1965 as a highly effective anticancer drug,[4] many cisplatin-type complexes of general formula [$PtCl_2$(N,N)][5–7] have been tested as alternative chemotherapeutics with the aim of reducing the serious side effects derived from the use of cisplatin (renal toxicity, neurotoxicity, myelosuppression, etc.).[8]

During the past decades, different strategies have been considered in order to enhance the cytotoxic activity and to reduce the side effects of cisplatin through modification of the pharmacokinetics and the mechanism of action of the respective Pt drugs.[6] The most recurrent approaches are: (a) the modification of the amine ligands, (b) the substitution of the chlorides by other anionic ligands, and (c) the use of Pt(IV) prodrugs.

With regard to the first strategy, the substitution of the NH_3 ligands by heterocyclic and alicyclic amines could reduce the toxicity of the platinum complexes[9] and, in particular, it has been described that the use of bulky amines prevents the deactivation of the platinum complexes in comparison with cisplatin by binding to thiols present in the cell, such as glutathione.[10–13] Different platinum(II) complexes of the type [$PtCl_2$(Hpybzi)] (Hpybzi = 2-(2-pyridyl)benzimidazole-based ligands) have been previously synthesized and tested as antiproliferative drugs in different cancer cell lines.[14–20] In these works, three types of modifications on these complexes have been probed with contrasting results: (1) introduction of substituents on the benzene ring of the benzimidazole moiety; (2) introduction of diverse functional groups on the imidazole ring (N-R); and (3) replacement of the chloride ligands by other anionic groups.

In particular, the placement of methyl groups in the benzimidazole scaffold decreases the antitumor activity compared to the complex with the unfunctionalized 2-(2-pyridyl)benzimidazole.[14,21]

Moreover, the introduction of alkyl chains with different terminal groups (C≡N, SO_3^-, PPh_3^+) in the imidazole ring, employed by Merlino,[18,22] Mansour[20] and some of us[19] to improve the solubility in water or the cellular uptake of the complexes, causes, in most of the cases, the sequestration of the platinum(II) complexes by serum albumin and other proteins reducing the bioavailability of the complexes to interact with the DNA of the cancer cells. Finally, the introduction of the flexible N-methylene-benzotriazole fragment in the imidazole group, provided platinum complexes with *in vitro* cytotoxic activity on human neuroblastoma cells (SH-SY5Y) comparable to that of cisplatin.[17]

On the other hand, the substitution of the chlorides by other anionic ligands has been less explored. Thus, the substitution of the chloride ligands in [$PtCl_2$(Hpybzi)] by iodide groups led

to a more active complex against the A2780 ovarian cell line in comparison to cisplatin.[16]

Combining two strategies, Chakravarty *et al.*[23] have introduced a BODIPY appended functional group in the 2-(2-pyridyl)benzimidazole scaffold, and catecholates as anionic ligands in a new type of Pt(II) derivative, with the aim to apply these complexes as PDT agents (Photo-Dynamic Therapy). These platinum complexes are cytotoxic under irradiation with visible light and are non-cytotoxic in the dark, which makes them suitable candidates for PDT. Irradiation of the complex generates ROS (Reactive Oxygen Species) *in vitro* provoking the mitochondrial membrane depolarization on HaCat human skin keratinocyte cells.

Inspired by these studies, we synthesized the first family of cyclometalated platinum(II) complexes that contains N-CH_2-aryl pyridylbenzimidazole scaffolds. The chosen design for our Pt complexes *a priori* provides the following benefits: (a) the presence of the 2-phenylpyridinate ligand could give us luminescent complexes with enhanced cytotoxicity under irradiation by generation of Reactive Oxygen Species (ROS); (b) the substitution of the NH group of the benzimidazole scaffold could modify the cytotoxicity and the cellular uptake, respect to the complex with Hpybzi, and avoid the sequestration of the platinum complexes by serum albumin proteins; and (c) the presence of the methylene group provides flexibility to the platinum(II) derivatives to adopt the right conformation to interact with DNA.

Herein, we describe the synthesis and characterization of a new family of neutral cyclometalated platinum complexes, their stability, photophysical properties and their cytotoxic activity in the adenocarcinoma colon cell line SW480. Additionally, we have also tested their biological activity in Gram positive and Gram negative bacteria strains of clinical interest. Moreover, we have analyzed the influence of different aromatic moieties (N-CH_2-Ar) on these properties.

RESULTS AND DISCUSSION

Synthesis and characterization in solution of the ligands L2-L4 and the complexes [Pt-L1]-[Pt-L4]

Ligands: 2-(2-Pyridyl)benzimidazole (**L1**, commercially available) was functionalized by deprotonation of the NH group of the imidazole fragment with K_2CO_3 followed by the addition of the corresponding arylalkyl bromide to obtain the desired ligands **L2-L4** (Scheme 1).[24]

Scheme 1. Synthesis of ancillary ligands L2-L4

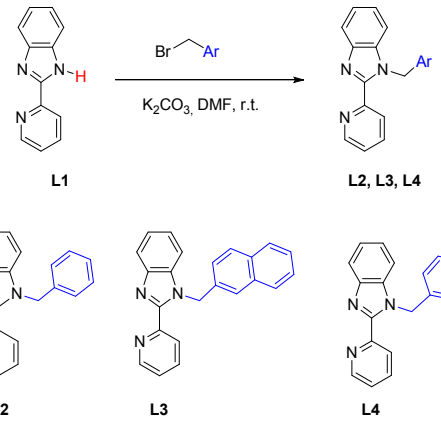

The new platinum complexes **[Pt-L1]-[Pt-L4]** with general formula [Pt(κ²-(**C^N**))Cl(κ¹-(**L**))] (where **C^N** = 2-phenylpyridinate and **L** = arylalkyl derivatives of 2-(2-pyridyl)benzimidazole) have been synthesized in two steps:

1.- *Synthesis of the platinum precursor*: the platinum precursor [κ²-(N^C)-(2-phenylpyridine)-κ¹-(N)-(2-phenylpyridine)chloro platinum(II)] **[Pt-0]** was synthesized following a described procedure[25] that involves the reaction of two equivalents of 2-phenylpyridine with K_2PtCl_4 as shown in Scheme 2 (see ^{1}H NMR spectrum in Figure SI1).

Scheme 2. Synthesis of platinum precursor [Pt-L0]

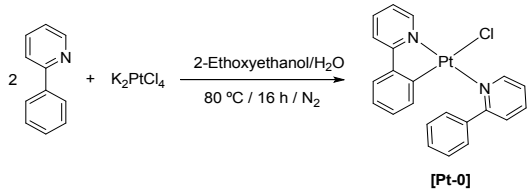

2.- *Coordination of the auxiliary ligands (**L1-L4**):* The cyclometalated complexes **[Pt-L1]-[Pt-L4]** were synthesized by reacting the platinum precursor **[Pt-0]** with ligands **L1-L4** in DMF at 65 °C or reflux for the required time (see

Scheme **3** and Experimental Section). ^{1}H NMR spectra and X-Ray diffraction studies of single crystals confirm that the obtained complexes **[Pt-L1]-[Pt-L4]** exhibit a κ^1 coordination mode for the 2-(2-pyridyl)benzimidazole based ligands involving the N atom of the imidazole ring in contrast with the expected κ^2-(N^N) coordination fashion[25] (see ORTEP diagrams in Figure 1). Hence, a chloride group completes the coordination sphere of the Platinum center. All the complexes are stable under atmospheric conditions.

Scheme 3. Synthesis of the Platinum complexes [Pt-L1]-[Pt-L4].

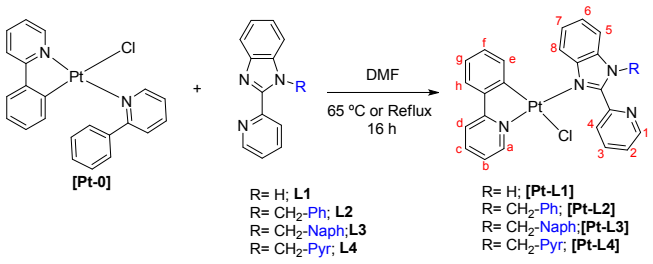

The ^{1}H NMR spectra of the new complexes **[Pt-L1]-[Pt-L4]** were recorded in $CDCl_3$ and exhibit two symptomatic features: (a) They show two doublets with the typical Pt-H coupling splitting for protons Ha ($^3J_{Pt-H}$= 36-38 Hz) and He ($^3J_{Pt-H}$= 42-44 Hz) whereas the peak attributed to H1 (**L1-L4**) lacks Pt-coupling features in agreement with a κ^1-N_{im} coordination mode; (b) The spectra of **[Pt-L2]-[Pt-L4]** display two mutually coupled doublets (J_{H-H}= 15-16 Hz) around 6 ppm for the diastereotopic CH_2 protons, which reveals the chiral nature of these derivatives as a result of restricted rotation about the Pt-N_{im} axis (axial chirality, see Experimental Section and Figure SI2 for **Pt-L3** as an example).

The HR-MS-ESI spectra in positive ion mode of **[Pt-L1]-[Pt-L4]** exhibited in each case a peak envelope fully compatible

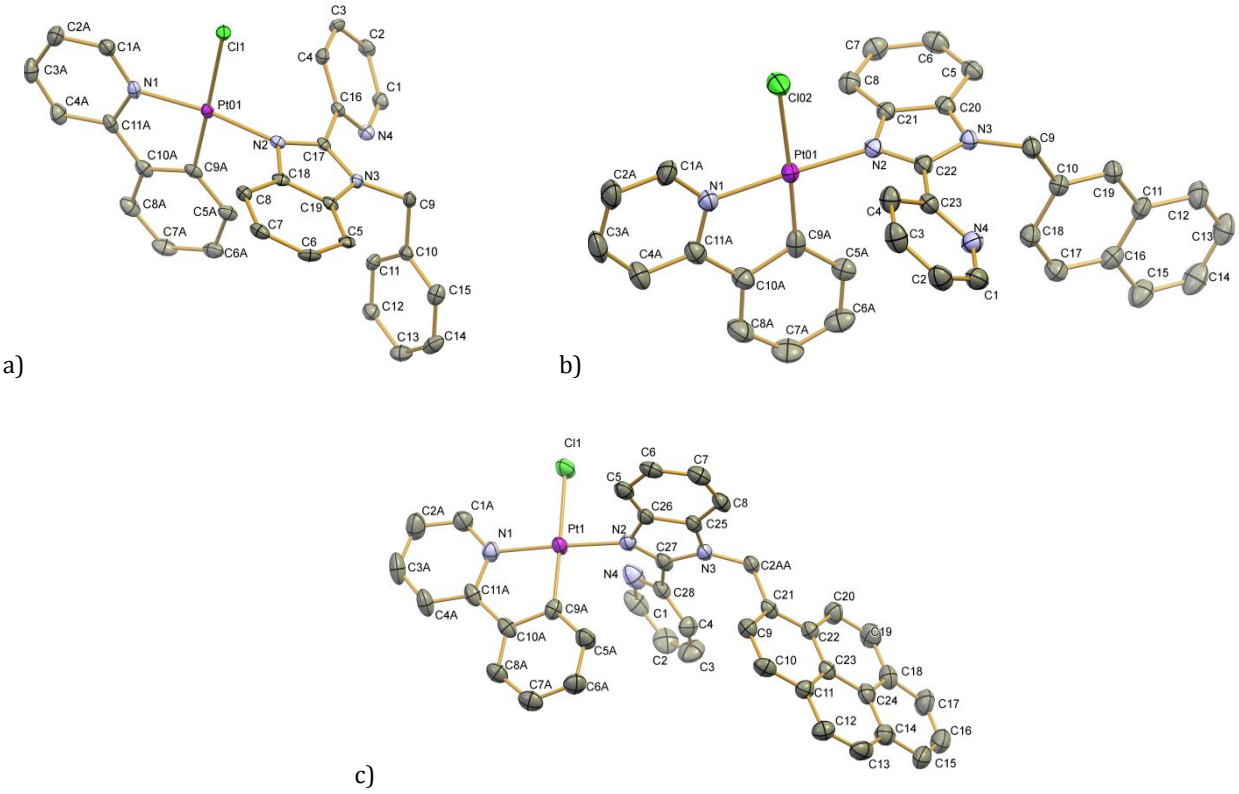

Figure 1. ORTEP diagrams for the platinum complexes forming part of the asymmetric unit of the crystal structure of: a) **[Pt-L2]**; b) **[Pt-L3]**; c) **[Pt-L4]**. Thermal ellipsoids are shown at the 30% probability level. Hydrogen atoms have been omitted for clarity.

(*m/z* ratio and isotopic pattern) with the respective cationic fragments [Pt(κ^2-(C^N))(κ^1-(**L**))]$^+$ in which the chloride anion has been lost (see Experimental Section and mass spectrum of **[Pt-L2]**, as an example, in Figure SI3).

Solid State Structure of the Pt(II) complexes

Single crystals suitable for X-Ray diffraction were obtained by slow evaporation of solutions of for **[Pt-L2]** and **[Pt-L3]** in acetone, or of **[Pt-L4]**. in CH_2Cl_2/Hexane (1:1). The ORTEP diagrams for **[Pt-L2]-[Pt-L4]** are depicted in Figure 1 and selected bond lengths and angles with estimated standard deviations are gathered in

Table 1 and Table 2, and crystallographic refinement parameters are given in the Supporting Information (Tables SI1, SI3 and SI5). In the complexes **[Pt-L2]-[Pt-L4]** the platinum center displays a slightly distorted square plane coordination geometry with a *trans*-N,N disposition for the N atom of the 2-phenylpyridinate ligand and the N atom of the imidazole fragment of the corresponding ligands **L2-L4**. Complexes **[Pt-L2]** and **[Pt-L3]** crystallize in the monoclinic space groups $P2_1/n$ and $P2_1/c$, respectively, and show two pairs of enantiomeric molecules in the unit cell, whereas complex **[Pt-L4]** crystallizes in the triclinic space group P-1 and displays one pair of enantiomeric molecules (atropoisomers) in the unit cell. In general, the Pt-N distances that define the distorted square planar geometry are quite similar (approx. 2 Å). Whereas, the distance Pt-Cl(1) observed for the complexes **[Pt-L2]-[Pt-L4]** are about 2.4 Å, comparable to those of related complexes[26,27] in which the Cl ligands are in *trans* to the sp^2 carbon of the 2-phenylpyridinate ligand. The bite angles C(9A)-Pt(1)-N(1) for all the complexes present values lower than 90°. The opposite angle N(2)-Pt(1)-Cl(1) present values between 88°-90° (see

Table **2**).

The bond distances and angles values are similar to those reported in the literature for [Pt(ppy)Cl(1-Methylimidazole)] and [Pt(ppy)Cl(4-Methylpyridine].[27]

Table 1. Selected bond lengths (Å) for the crystal structure of complexes [Pt-L1]-[Pt-L4].

Distances (Å)	[Pt-L2]	[Pt-L3]	[Pt-L4]
Pt(1)-Cl(1)	2.4196(10)	2.4112(14)	2.411(11)
Pt(1)-N(1)	2.011(3)	2.007(4)	2.007(3)
Pt(1)-N(2)	2.024(3)	2.031(4)	2.012(7)
Pt(1)-C(9A)	1.979(4)	1.920(6)	1.970(8)

The 3D-structures of **[Pt-L2]** and **[Pt-L3]** are stabilized by double hydrogen bonds of the type CH---Cl---HC that involve the chloride ligand of one molecule and two C-H groups belonging to aromatic rings of neighboring molecules (see Figures SI4, SI7 and Table SI7). Moreover, different CH-π interactions are observed in the crystal structure of these two complexes**.** These interactions are resumed in the supporting information (Figures SI5, SI6, SI8 and SI9, and Tables SI2 and SI4).

In the crystal structure of **[Pt-L4]** we observe hydrogen bonding interactions of the type CH---Cl concerning the Cl^- ligand of one molecule and the methylene group of a neighbouring molecule (see Figure SI10 and Table SI7). Several CH-π interactions are observed in this case, for instance, between the methylene group and the benzimidazole fragment, and two more between two ppy^- ligands and the benzimidazole fragment (see Figures SI11, SI12b and Table SI6). The structure presents two different π–π stacking interactions, the first, between two ppy^- fragments and the second, between two pyrene scaffolds of different molecules (see Figures SI11-SI12 and Table SI6).

Table 2. Selected angles (°) for the crystal structure of the complexes [Pt-L2]-[Pt-L4].

Angles (°)	[Pt-L2]	[Pt-L3]	[Pt-L4]
N(2)-Pt(1)-N(1)	172.25(14)	174.78(17)	175.26(2)
C(9A)-Pt(1)-Cl(1)	175.70(12)	177.47(17)	177.5(2)
N(1)-Pt(1)-Cl(1)	96.42(11)	95.96(14)	95.1(2)
N(2)-Pt(1)-Cl(1)	90.42(10)	88.44(12)	88.57(18)
C(9A)-Pt(1)-N(1)	81.37(17)	81.6(12)	83.1(3)
C(9A)-Pt(1)-N(2)	92.03(16)	93.99(19)	93.3(3)

Stability of the complexes [Pt-L1]-[Pt-L4] in solution

For the biological studies, the solubility of the complexes in aqueous solution is essential. Due to the low solubility of the Pt(II) complexes in water, the solvent mixture H_2O/DMSO was selected. Thus, we studied the stability of **[Pt-L1]-[Pt-L4]** in DMSO-d_6 by ^{1}H NMR spectroscopy (see Figures SI13-SI16). After the solubilization of complexes **[Pt-L1]-[Pt-L4]** in DMSO-d_6 ($4{\cdot}10^{-3}$ M) the corresponding ^{1}H NMR spectra revealed the presence of free ligands, **L1-L4**, from the very beginning, and after 3 hours the dissociation of the ligands is almost complete (>95%).

Due to the low stability of the platinum complexes in DMSO-d_6 and taking into account the previous cytotoxicity studies on Platinum(II) complexes performed in DMF/water solutions by several groups,[28,29] we also analyzed the stability of our complexes in DMF-d_7 by ^{1}H NMR (see Figures SI17-SI20). Consequently, we determined that the stability of complexes **[Pt-L1]-[Pt-L4]** in DMF-d_7 after 24 hours is higher than in DMSO-d_6. However, we also observed the appearance of free ligands (**L1-L4**) in this solvent (5 % for **[Pt-L1]**, 7% for **[Pt-L2],** 6% for **[Pt-L3]** and 57% for **[Pt-L4]** after 24 h).

To study the behavior of the complexes in presence of water, the addition of 100 μL of D_2O over the solutions

prepared for studying the stability in DMF (final ratio DMF-d_7/D_2O (4:1) and final concentration of Pt complexes $5{\cdot}10^{-3}$ M), did not provoke the substitution of the chloride ligand by a water molecule (see Figures SI21-SI24). On the contrary, we observed again, by ^{1}H NMR spectra, the dissociation of the ancillary ligands **L1 (**23 % after 24 h), **L2** (9% after 72 h) and **L3** (18% after 48 h) from the respective complexes. The addition of D_2O over the solution of **[Pt-L4]** in DMF-d_7 provoked the precipitation of the free ligand **L4** present in the solution, and the signals of **L4** disappeared fully in the ^{1}H NMR spectrum. In order to corroborate that the substitution of the chloride atom by a water molecule had not taken placed, $AgNO_3$ was added forcing the release of the chloride and the ^{1}H NMR spectra of the aqua-complex formed were recorded. The comparison of both spectra, before and after the addition of the $AgNO_3$, showed different species that rule out that the substitution of the chloride by a water molecule (see Figures SI25-SI28 in S.I.).

Additionally, we tested the stability of our complexes in NaCaC (2.5 mM, pH=7): DMF mixtures, used in the biological assays. Due to the low solubility of the platinum complexes **[Pt-L1]-[Pt-L4]** in mixtures DMF-d_7/D_2O with high content in D_2O and the impossibility of register their spectra due to precipitation, we analyzed their stability by HR-MS spectrometry (see experimental section). All the complexes are stable after 24h in solution of DMF/NaCaC (DMF 2%) (see NaCaC chromatogram in Figure SI29 and chromatogram of **[Pt-L1]-[Pt-L4]** Figures SI30-SI33) and free ligands **L1-L4** are not observed in any case.

Photophysical properties

The UV-Vis absorption spectra of ligands **L1-L4** and complexes **[Pt-L1]-[Pt-L4]** were recorded in DMF solutions (10^{-5} M) at 25 °C. The absorption spectra of the ligands **L1-L4** in DMF are compiled in Figure SI34 and data in Table SI8. Ligands **L1-L3** present broad absorption bands centered at 310-313 nm, while **L4** present intense and well-defined characteristic bands of pyrene moieties.

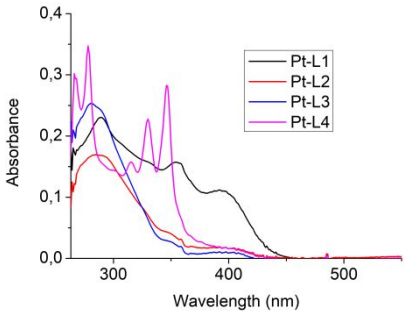

Figure 2. UV-Vis absorption spectra of the complexes **[Pt-L1]- [Pt-L4]** (10^{-5} M) at 25 °C in DMF.

The absorption spectra of the complexes **[Pt-L1]-[Pt-L3]** in solution of DMF (see Figure 2) feature broad absorption bands and the complex **[Pt-L4]** presents well-defined absorption bands influenced by the pyrenyl substituent. The maximum of the absorption bands of **[Pt-L1]-[Pt-L4]** are located between 278-297 nm (see Table 3). These bands are attributed to singlet spin-allowed ligand centered transitions ($\pi \rightarrow \pi^*$ ^{1}LC) taking place in both the **L1-L4** and the phenylpyridinate ligands. Moreover, a new band is observed in the spectra of the platinum complexes centered between 395-407 nm that could be assigned to spin-allowed metal to ligand charge transfer ^{1}MLCT transitions (see Table 3).

Table 3. Electronic properties of the platinum complexes **[Pt-L1]-[Pt-L4]** measured and DMF (10^{-5} M) at 25 °C.

Complex	Solvent	λ_{abs} (nm)	$\varepsilon \cdot 10^{-3}$ ($M^{-1}{\cdot}cm^{-1}$)
[Pt-L1]	DMF	289*, 354, 397¥	23.04, 15.75, 11
[Pt-L2]	DMF	287*, 352(s), 401¥	23.04, 3.76, 1.56
[Pt-L3]	DMF	280*, 352, 395¥	25.31, 2.5, 0.86
[Pt-L4]	DMF	266, 278*, 315, 330, 346, 403¥	30.18, 34.71, 15.75, 22.75, 28.29, 1,58

*maximum ¥ center of a broad band

The emission spectra of the complexes **[Pt-L1]-[Pt-L4]** were recorded for 10^{-5} M solutions in deoxygenated DMF at 25 °C. Unfortunately, the platinum complexes have not emissive properties. This fact could be attributed to the lower structural rigidity[30] of our platinum complexes compared with other phenylpyridinate-Pt complexes like [Pt(ppy)(bpy)]Cl.[31]

Biological Activity

The biological activity of ligands **L1-L4** and complexes **[Pt-L1]-[Pt-L4]** was explored in terms of antitumor and antimicrobial activity in mixtures water/DMF (lower than 2% of DMF).

Antimicrobial activity : Regarding the antibacterial activity, the auxiliary ligands **L1-L4** and their corresponding **[Pt-L1]-[Pt-L4]** complexes were tested in bacteria of clinical interest, *E. faecium* and *S. aureus* (Gram positive bacteria), *A. baumannii* and *P. aeruginosa* (Gram negative bacteria), with Ampicillin as positive control. Unfortunately, neither of the ligands or the platinum complexes are active against these bacteria. (see Table SI9).

Anticancer activity: With regard to the antitumor activity, the half-maximal inhibitory concentration (IC_{50}) values of the ligands **L1-L4** and complexes **[Pt-L1]-[Pt-L4]** against SW480 (colon adenocarcinoma) cells was determined by the MTT Assay (see Table 4) after 24 h and 72 h. Neither the ligands **L1-L4** nor the complex **[Pt-L4]** showed cytotoxicity upon bith periods of time. After 24 h of treatment only **[Pt-L1]** and **[Pt-L2]** are cytotoxic towards

SW480 cells, while **[Pt-L3]** present cytotoxicity after 72 h. Important morphological changes (apoptotic bodies and vacuoles formation) were observed in SW480 cells treated with **[Pt-L1]**-**[Pt-L3]** (Figure SI35) after 72 h of treatment. **[Pt-L1]** and **[Pt-L2]** are cytotoxic in dose and time-dependent manners being at least two-fold more cytotoxic than cisplatin. The IC_{50} value of [**Pt-L3]** at 72 h cannot be determined due to its low solubility but a significant decrease in the survival rate of SW480 cells at 15 μM was observed. Additionally, the Pt(II) complexes were irradiated with UV light (λ= 365 nm) to test the effect of the irradiation in the behaviour of the complexes. The irradiation did not provoke any IC_{50} variation.

Table 4. Cytotoxic activity of the ligands **L1-L4** and the complexes **[Pt-L1]-[Pt-L4]** against SW480 cancer cells upon 24 h and 72 h of exposure time. Cisplatin is included for comparison purposes.

	IC_{50} (μM), 24h	IC_{50} (μM), 72h
[L1]	n.e.	n.e.
[L2]	n.e.	n.e.
[L3]	n.e.	n.e.
[L4]	n.e.	n.e.
[Pt-L1]	19.9 ± 1.2	3.9 ± 0.6
[Pt-L2]	16.6 ± 0.5	7.8 ± 0.9
[Pt-L3]	n.e.	> 15
[Pt-L4]	n.e.	n.e
Cisplatin	38.9 ± 2.0	15.3 ± 1.6

n.e.: no effect was observed for all tested concentrations.

Interaction of the Pt(II) complexes with biomolecules and cellular uptake

Traditionally, it has been propose that DNA is the main target of cisplatin, but also several proteins or enzymes have been involved in the pharmacological action of different platinum drugs.[32] Thus, the binding properties to relevant biomolecules such as *d*GMP, DNA and BSA, as well as, the cellular uptake have been studied for the **[Pt-L1]**-**[Pt-L4]** in order to establish which factors are determining to their cytotoxicity.

Cellular uptake and BSA interactions: Metal accumulation of the platinum(II) complexes **[Pt-L1]-[Pt-L4]** inside SW480 cells was determined by ICP-MS (Figure 3). All the complexes are internalized more than cisplatin, and consistently, the more cytotoxic derivatives, **[Pt-L1]** and **[Pt-L2]**, feature the higher accumulation values inside the cells. Interestingly, although the cellular uptake of **[Pt-L4]** is similar to that of the cytotoxic complexes (**[Pt-L1]** and **[Pt-L2]**), this derivative is non-cytotoxic.

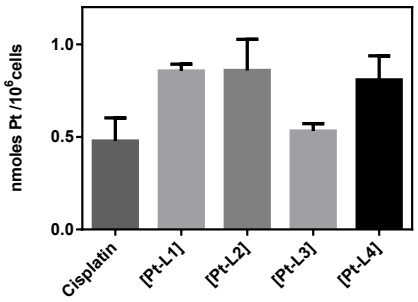

Figure 3. Metal accumulation in SW480 cells after 24 h of exposure to 2 μM of complexes **[Pt-L1]-[Pt-L4]**.

In an attempt to explain the lack of correlation between cytotoxicity and cellular accumulation of the complexes, the interaction with bovine serum albumin (BSA) was explored due to its structural resemblance with human serum albumin (HSA).[33] Blood plasma proteins, predominantly serum albumin, governs the transport of metal ions and xenobiotics through the bloodstream. Therefore, the binding of the complexes to serum albumin may govern the drug availability and consequently its biological activity. According to the results from native electrophoresis experiments, none of the Pt-complexes interact with BSA (Figure SI36).

dGMP and DNA binding ability: The ability of the Pt(II) complexes to interact with *d*GMP was studied in solution of DMF-d_7/D_2O by ^1H and $^{31}P\{^1H\}$ NMR (see Experimental Section). Among the complexes **[Pt-L1]-[Pt-L4]**, complex **[Pt-L1]** interacts in a fast manner with the nucleotide by covalent binding through the N7 leading a downfield shift of the H8 signal (see Figure SI37). Simultaneously, a new downfield shifted signal in the ^{31}P NMR spectrum appeared ($\Delta\delta(^{31}P)$=0.69 ppm), which confirms the binding to *d*GMP through N7 (see Figure SI38).[34,35] The Pt-OPO_3 isomers were not observed ($\Delta\delta(^{31}P)$ >1 ppm and ^{31}P signals with satellites are expected for them).[34,35] In contrast, for **[Pt-L2]** the Pt-N7-*d*GMP adduct is only observed by ^{31}P NMR, since the ^1H NMR exhibits non-well defined signals (a solid appear in the NMR tube, see Figures SI39-SI40). The $\Delta\delta(^{31}P)$ = 0.7 ppm indicates that the formation of the Pt-N7-*d*GMP adduct requires longer times (more than 7h) than in the case of **[Pt-L1]**.[34,35] Finally, the complexes **[Pt-L3]** and **[Pt-L4]** did not interact covalently with *d*GMP (see Figures SI41-SI44), probably due to an steric effect associated to the bulky condensed aromatic rings.

In order to confirm the ability of these complexes to interact covalently with DNA, the effect of the complexes **[Pt-L1]-[Pt-L4]** on the electrophoretic mobility of the plasmid of DNA pUC18 was studied (see Figure 4).

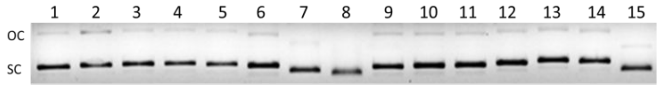

Figure 4. Agarose gel electrophoresis of the pUC18 plasmid incubated overnight with different concentrations of the Pt complexes. Lane 1: pUC18 alone, lane 2: pUC18 + 2% DMF, lanes 3-5: pUC18 + **[Pt-L1]** at [complex]/[DNA] ratio 1, 10 and 20; lanes 6-8: pUC18 + **[Pt-L2]** at [complex]/[DNA] ratio 1, 10 and 20; lanes 9-11: pUC18 + **[Pt-L3]** at [complex]/[DNA] ratio 1, 10 and 20; lanes 12-14: pUC18 + **[Pt-L4]** at [complex]/[DNA] ratio 1, 10 and 20; lane 15: cisplatin at [cisplatin]/[DNA] ratio = 10. C_{DNA} = 20 μM, OC (open circular) and SC (supercoiled).

As previously has been observed, the migration rate of SC (supercoiled) form of pUC18, in presence of cisplatin, depends of the [cisplatin]/[DNA] ratio.[36] The effect of **[Pt-L2]** on the DNA conformation observed in electrophoresis at **[Pt-L2]**/[DNA] = 1, 10 and 20 (lanes 6, 7 and 8, Figure 4) is comparable to that induced by cisplatin at the same [cisplatin]/[DNA] ratio (see Figure SI45). As occurs with cisplatin, the SC (supercoiled) form of the pUC18 plasmid migrates faster at higher **[Pt-L2]** concentrations (lines 7 and 8, Figure 4) than in the absence of the Pt complex (lanes 1 and 2, Figure 4), while there is no variation in the rate migration at **[Pt-L2]** /[DNA] = 1(line 6).

Thus, the effect of **[Pt-L2]** on the DNA conformation observed in electrophoresis is comparable to that induced by cisplatin. This behavior in conjunction with time-dependent CD experiments (Figure 5) indicates that **[Pt-L2]** complex binds covalently to DNA. In consequence, DNA interaction could be responsible for its high cytotoxicity**.**

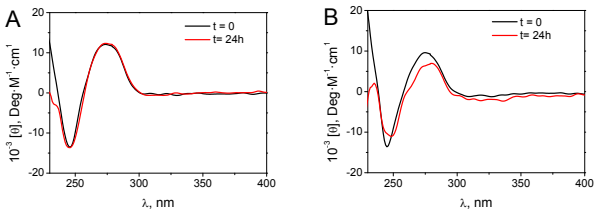

Figure 5. CD spectra of DNA in the absence and in the presence of **[Pt-L1]** (A) and **[Pt-L2]** (B), t = 0 and 24h. [DNA] = 5×10^{-5} M, [DNA]/[Pt complexes] = 1, pH = 7 and T=25°C.

On the other hand, the retardation in the migration of the SC form observed in the presence of **[Pt-L4]** (lanes 12, 13 and 14) points to intercalation as the binding mode between **[Pt-L4]** and DNA,[37] probably through the pyrenyl moiety. However, **[Pt-L4]** is non-cytotoxic in contrast to several drugs that display this biological mode of action.[38,39] Interestingly, no effect on the plasmid migration was observed with **[Pt-L3]** and with the cytotoxic complex **[Pt-L1]** (see lanes 3-5 for **[Pt-L1]** and 9-11 for **[Pt-L3]**). Although $^{31}P\{^1H\}$ and ^1H NMR experiments showed covalent binding between N7-*d*GMP and **[Pt-L1]**, the electrophoresis and the absence of conformational changes in DNA observed in CD experiments, indicated that covalent binding with DNA is absent. These results confirm that the mode of action of **[Pt-L1]** is not related to DNA binding, and other targets[40] and a different molecular mechanism could be involved.[41,42]

Conclusions

The first family of neutral cyclometalated platinum(II) complexes derived from the 2-(2-pyridyl)benzimidazole scaffold have been synthesized and fully characterized in solution and in solid state. The unexpected κ^1 coordination mode of the 2-(2-Pyridyl)benzimidazole-derived ligands to the metal centre led to axially chirality complexes, which are non-emissive in solution probably due to the lack of structural rigidity. The aromatic moieties bounded to the nitrogen atom of the imidazole fragment have a great influence on the cytotoxic activity of the Pt(II) complexes **[Pt-L1]-[Pt-L4]** and on the mode of interaction of the latter with DNA. Thus, the platinum complexes **[Pt-L1]** and **[Pt-L2],** with the smaller substituents in the nitrogen of the imidazole, are at least 2-fold more cytotoxic than cisplatin in SW480 cells and, even though both are able to bind to *d*GMP, only **[Pt-L2]** bind covalently to DNA inducing the same conformational changes in the pUC18 plasmid than cisplatin. Complex **[Pt-L3]** showed low activity at long times (72h) and the complex **[Pt-L4]** with the bulkiest aromatic moiety does not present cytotoxicity, although **[Pt-L4]** showed intercalation into DNA. Neither of the platinum (II) complexes present interaction with BSA showing all of them higher internalization than cisplatin in the SW480 cancer cells.

EXPERIMENTAL SECTION

Starting materials. K_2PtCl_4 was purchased from Strem chemicals and used as received. The starting complex κ^2(N^C)-(2-phenylpyridine)-κ^1(N)-(2-phenylpyridine)chloro platinum(II) was prepared according to the reported procedure.[25] 2-(2-Pyridyl)benzimidazole (**L1**) was purchased from Sigma-Aldrich and used without further purification and 2-phenylpyridine and aromatic bromomethyl derivatives were obtained from Sigma-Aldrich and used as received. Deuterated solvents ($CDCl_3$, D_2O, DMSO-d_6, and DMF-d_7) were obtained from Eurisotop.

Synthesis and Characterization: *Syntheses of κ^2(N^C^2)-(2-phenylpyridine)-κ^1(N)-(2-phenylpyridine)chloro platinum(II),* ***[Pt-0]:*** K_2PtCl_4 (1.34 g, 3.22 mmol) was dissolved in 25 mL of a mixture of Ethoxyethanol/H_2O (3:1) and stirred for 10 min. Then, 2-phenylpyridine (920 μL, 6.44 mmol) was added over the previous solution and the reaction mixture was stirred at 80 °C for 16 h. After this time, the solvents were removed under vacuum and the obtained solid was washed with MeOH (3x 10 mL) and pentane (2 x 5 mL), filtered and dried under vacuum. Yellow solid (1.46 g, 84 % yield). **^{1}H NMR (400 MHz, $CDCl_3$):** δ 9.62 (d, J = 5.90, $J_{Pt\text{-}H}$ = 20.2 Hz, 1H), 9.25 (d, J = 5.87, $J_{Pt\text{-}H}$ = 22.7 Hz, 1H), 8.09 (m, 2H), 7.94 (td, J = 7.9, 1.6 Hz, 1H), 7.74 (td, J = 7.8, 1.6 Hz, 1H), 7.63 (d, J = 7.9 Hz, 1H), 7.52 (d, J = 7.8 Hz, 1H), 7.37 (ddd, J = 8.4, 5.9, 1.5 Hz, 1H), 7.32 (m, 4H), 7.07 (td, J = 7.4, 1.4 Hz, 1H), 6.99 (td, J = 7.6, 1.1 Hz, 1H), 6.87 (td, J = 7.5, 1.3 Hz, 1H), 6.19 (d, J = 7.7 Hz, $J_{Pt\text{-}H}$ = 24.2 Hz, 1H). **HR-MS (*m/z*):** [M - Cl]$^+$ calcd for $[C_{22}H_{17}N_2Pt]^+$, 504.1041; found, 504.1044.

*1-benzyl-2-(pyridin-2-yl)-1H-benzo[d]imidazole (**L2**):*[24] 2-(2-Pyridyl)benzimidazole (**L1**) (350 mg, 1.79 mmol) and K_2CO_3 (495.56 mg, 3.59 mmol) were dissolved in 7 mL of DMF and the mixture was stirred for 30 min. at room temperature. Then, the benzyl bromide (277 μL, 2.33 mmol) was added, and the reaction

mixture was stirred at room temperature for 18 h. The solvent was evaporated under reduced pressure, washed with water (2 x 7 mL) and Et_2O (2 x 5 mL), filtered and dried under vacuum. Pale beige solid (263 mg, 51 % yield). **^{1}H NMR (400 MHz, $CDCl_3$):** δ 8.63 (d, *J* = 4.8 Hz, 1H), 8.45 (d, *J* = 8.1 Hz, 1H), 7.85 (m, 2H), 7.25 (m, 9H), 6.20 (s, 2H). **^{13}C NMR {^{1}H} (101 MHz, $CDCl_3$)**: δ 150.53 (Cq), 149.59 (Cq), 148.95 (CH_{arom}), 137.70 (2Cq), 137.02 (CH_{arom}), 136.85(Cq), 128.89 (2 CH_{arom}), 127.66 (CH_{arom}), 127.11 (2 CH_{arom}), 125.08 (CH_{arom}), 124.22 (CH_{arom}), 123.94 (CH_{arom}), 123.19 (CH_{arom}), 120.37 (CH_{arom}), 111.11 (CH_{arom}), 49.26 (CH_2). **HR-MS (*m/z*):** [M + H]$^+$ calcd for $[C_{19}H_{16}N_3]^+$, 286.1342; found, 286.1346. **Elemental analysis**: calcd for $C_{19}H_{15}N_3$: C, 79.98; H, 5.30; N, 14.73; found C, 80.12; H, 5.22; N, 14.43.

*1-(naphthalen-2-ylmethyl)-2-(pyridin-2-yl)-1H-benzo[d]imidazole, (**L3**):*[43] Ligand **L3** was prepared as previously described for **L2**, from 2-(2-Pyridyl)benzimidazole (**L1**) (350 mg, 1.79 mmol), K_2CO_3 (495.56 mg, 3.59 mmol) and 2-(bromomethyl)naphthalene (515.30 mg, 2.33 mmol). Beige solid (394 mg, 65 % yield).**^{1}H NMR (400 MHz, $CDCl_3$):** δ 8.62 (ddd, *J* = 4.9, 1.7, 0.8 Hz, 1H), 8.46 (d, *J* = 8.0, 1.1 Hz, 1H), 7.88 (d, *J* = 8.1 Hz, 1H), 7.83 (td, *J* = 7.8, 1.8 Hz, 1H), 7.77 (dd, *J* = 6.1, 3.4 Hz, 1H), 7.74 (d, *J* = 8.6 Hz, 1H), 7.68 (*J* = 6.2, 3.3 Hz, 1H), 7.55 (br s, 1H,), 7.41 (m, 2H), 7.36 (m, 1H), 7.31 (m, 3H), 7.23 (m, 1H), 6.36 (s, 2H). **^{13}C{^{1}H}(101 MHz, $CDCl_3$)**: δ 150.71 (C_q), 150.16 (C_q), 148.78 (CH_{arom}), 142.93 (C_q), 137.00 (CH_{arom}), 135.11 (C_q), 133.39 (C_q), 132.82 (C_q), 128.54 (CH_{arom}), 127.91 (CH_{arom}), 127.77 (CH_{arom}), 126.32 (CH_{arom}), 125.98 (CH_{arom}), 125.50 (CH_{arom}), 125.01 (CH_{arom}), 124.83 (CH_{arom}), 124.00 (CH_{arom}), 123.76 (CH_{arom}), 122.98 (CH_{arom}), 120.30 (CH_{arom}), 110.94 (CH_{arom}), 49.30 (CH_2). **HR-MS (*m/z*):** [M + H]$^+$ calcd for $[C_{23}H_{18}N_3]^+$, 336.1495; found, 336.1505. **Elemental analysis:** calcd for $C_{23}H_{17}N_3 \cdot (H_2O)_{0.5}$= C, 80.21; H, 5.27; N, 12.22; found C, 80.10; H, 4.81; N, 11.82.

1-(pyren-1-ylmethyl)-2-(pyridin-2-yl)-1H-benzo[d]imidazole, (**L4**):[43] Ligand **L4** was synthesized as described for **L2**, from 2-(2-Pyridyl)benzimidazole (**L1**) (250 mg, 1.28 mmol), K_2CO_3 (176.99 mg, 1.28 mmol) and 1-(bromomethyl)pyrene (378 mg, 1.28 mmol). Beige solid (208 mg, 40 % yield). **^{1}H NMR (400 MHz, $CDCl_3$):** δ 8.50 (d, *J* = 8.0 Hz, 1H), 8.47 (d, *J* = 9.3 Hz, 1H), 8.42 (d, *J* = 4.5 Hz, 1H), 8.25 (m, 1H), 8.23 (d, *J* = 3.9 Hz, 1H), 8.20 (d, *J* = 7.5 Hz, 1H), 8.04 (m, 2H), 7.97 (s, 1H), 7.95 (d, J = 2.97 Hz), 7.92 (d, J = 8.4 Hz, 1H), 7.79 (td, J = 7.8, 1.8 Hz, 1H), 7.34 (td, J = 7.4, 1.3 Hz, 1H), 7.25 (m, 1H), 7.28 (m, 2H), 6.96 (s, 2H).**^{13}C{^{1}H}(101 MHz, $CDCl_3$)**: δ 150.62 (C_q), 150.50 (C_q), 148.81 (CH_{arom}), 142.99 (C_q), 137.29 (C_q), 136.94 (CH_{arom}), 131.53 (C_q), 130.86 (C_q), 130.78 (C_q), 130.59 (C_q), 128.17 (CH_{arom}), 127.78 (C_q+ CH_{arom}), 127.58 (CH_{arom}), 127.30 (CH_{arom}), 126.20 (CH_{arom}), 125.57 (CH_{arom}), 125.34 (CH_{arom}), 125.18 (CH_{arom}), 124.94 (2 C_q), 124.67 (CH_{arom}), 123.92 (CH_{arom}), 123.87 (CH_{arom}), 123.65 (C_q), 123.09 (CH_{arom}), 122.11 (CH_{arom}), 120.41 (CH_{arom}), 110.89 (CH_{arom}), 47.15 (CH_2). **HR-MS (*m/z*):** [M + H]+ calcd for $[C_{29}H_{20}N_3]$, 410.1657; found, 410.1662. **Elemental analysis:** calcd for $C_{29}H_{19}N_3 \cdot (H_2O)_{0.5}$= C, 83.23; H, 4.82; N, 10.04; found C, 83.52; H, 4.52; N, 9.73.

*Synthesis of [Pt(ppy)Cl(**L1**)], **[Pt-L1]**:* Platinum precursor **[Pt-0]** (100 mg, 185.21 µmol) and 2-(2-Pyridyl)benzimidazole (**L1**) (36 mg, 185.21 µmol) were dissolved in 10 mL of DMF and heated at 65 °C for 24 h. Then, the solvent was evaporated to dryness and the solid was washed with Et_2O under stirring, filtered and dried under vacuum. Yellow solid (49.5 mg, 47% yield). **^{1}H NMR (400 MHz, $CDCl_3$):** δ 11.14 (br s, 1H; NH), 10.65 (d, $J_{H\text{-}H}$ = 8.0 Hz, 1H; H1), 9.87 (d, $J_{Pt\text{-}H}$= 37.1, $J_{H\text{-}H}$ = 5.3 Hz, 1H), 8.63 (d, $J_{H\text{-}H}$ = 4.5 Hz, 1H; H_{arom}), 8.34 (d, $J_{H\text{-}H}$ = 7.5 Hz, 1H; H4), 7.90 (t, $J_{H\text{-}H}$ = 7.8 Hz, 1H; Hc), 7.82 (t, $J_{H\text{-}H}$ = 7.8 Hz, 1H; H2), 7.72 (t, $J_{H\text{-}H}$ = 7.8 Hz, 1H; H3), 7.57 (d, $J_{H\text{-}H}$ = 8.0 Hz, 1H; Hd), 7.47 (d, $J_{H\text{-}H}$ = 8.0 Hz, 1H; Hh), 7.36 (m, 3H; 3 H_{arom}), 7.23 (m, 1H; Hb), 7.01 (t, $J_{H\text{-}H}$ = 7.6 Hz, 1H; Hg), 6.74 (t, $J_{H\text{-}H}$ = 7.5 Hz, 1H; Hf), 6.19 (d, $J_{Pt\text{-}H}$= 43.3, $J_{H\text{-}H}$ = 8.06 Hz, 1H; He). **^{13}C{^{1}H} NMR (101 MHz, $CDCl_3$):** δ 167.6 (C_q), 151.3 (CH_{arom}), 149.2 (CH_{arom}), 138.8 (CH_{arom}), 137.5 (CH_{arom}), 130.2 (CH_{arom}), 129.1 (CH_{arom}), 128.9 (CH_{arom}), 127.0 (CH_{arom}), 125.9 (CH_{arom}), 125.7 (CH_{arom}), 124.1 (2 CH_{arom}), 123.4 (2 CH_{arom}), 118.8 (CH_{arom}), 11138 ppm (CH_{arom}). Due to the low resolution of the spectra, the rest of the quaternary carbons couldn't be assigned. **FT-IR (ATR) selected bands** 3262 (ν_{NH}), 1607-1581 ($\nu_{C=N,\ Py}$), 1467-1460($\nu_{C=N,\ imid}$), 556-501 ($\nu_{Pt\text{-}N}$) cm^{-1} **HR-MS (*m/z*):** [M - Cl]$^+$ calcd for $[C_{23}H_{17}N_4Pt]^+$: 544.1103; found 544.1096. **Elemental analysis**: calcd for $C_{23}H_{17}ClN_4Pt \cdot (H_2O)$= C, 46.20; H, 3.20; Cl, N, 9.37; found C, 46.29; H, 3.23; N, 8.91.

*Synthesis of [Pt(ppy)Cl(**L2**)], **[Pt-L2]**:* Platinum precursor **[Pt-0]** (94.6 mg, 175.23 µmol) and ligand **L2** (50 mg, 175.23 µmol) were dissolved in 10 mL of DMF and heated under reflux for 24 h. Then, the solvent was evaporated to dryness and the solid was washed with Et_2O (2 x 10 mL) under stirring and recrystallized in $CHCl_3$ in the freezer (5 mL), filtered and dried under vacuum. Pale yellow solid (63.5 mg, 54% yield). **^{1}H NMR (400 MHz, $CDCl_3$):** *δ* 9.80 (d, $J_{Pt\text{-}H}$= 36.2, $J_{H\text{-}H}$ = 5.9 Hz, 1H; Ha), 9.37 (d, $J_{H\text{-}H}$ = 7.96 Hz, 1H; H1), 8.64 (d, $J_{H\text{-}H}$ = 4.80 Hz, 1H; H4), 8.34 (m, 1H; H_{arom}), 7.81 (m, 2H; H2, Hc), 7.60 (d, $J_{H\text{-}H}$ = 8.08 Hz, 1H; Hd), 7.34 (m, 8H; Hh, 7H_{arom}), 7.22 (d, $J_{H\text{-}H}$ = 6.99 Hz, 2H; H3, H8), 7.16 (m, 1H; H7), 6.97 (t, $J_{H\text{-}H}$ = 7.53 Hz, 1H; Hb), 6.79 (t, $J_{H\text{-}H}$ = 7.48 Hz, 1H; Hg), 6.21 (d, $J_{Pt\text{-}H}$= 44.5, $J_{H\text{-}H}$ = 7.69 Hz, 1H; He), 5.92 ppm (d, $J_{H\text{-}H}$ = 15.9 Hz, 1H, C*H*-Ph), 5.85 ppm (d, $J_{H\text{-}H}$ = 15.7 Hz, 1H, CH*H*-Ph). **^{13}C{^{1}H} NMR (101 MHz, $CDCl_3$)**: *δ* 167.6 (C_q), 151.2 (Ca), 150.3 (C_q), 148.8 (C4), 148.1 (C_q), 144.5 (C_q), 141.1 (C_q), 140.6 (C_q), 138.5 (C2), 136.8 (Cc), 135.8 (C_q), 134.4 (C_q), 131.6 (Ce), 130.1 (Cf), 129.4 (2 CH_{arom}), 128.2 (C1), 128.1 (CH_{arom}), 127.1 (C7,CH_{arom}), 125.5 (C3 o C8), 125.1 (C3 o C8), 124.4 (CH_{arom}), 123.3 (CH_{arom}), 123.1 (Cg), 121.9 (Cb), 121.5 (CH_{arom}), 118.1 (Cd), 111.3 (CH_{arom}), 48.6 ppm (CH_2). **FT-IR (ATR) selected** 1607-1585 ($\nu_{C=N}$, Py), 1470-1444($\nu_{C=N}$, imid), 557-501 (νPt-N) cm^{-1} **HR-MS (*m/z*)**: [M - Cl]$^+$ calcd for $[C_{30}H_{23}N_4Pt]^+$, 634.1570; found, 634.1566. **Elemental analysis**: calcd for $C_{30}H_{23}ClN_4Pt \cdot (H_2O)$ = C, 52.37; H, 3.66; N, 8.14; found C, 52.12; H, 3.80; N, 7.79.

*Synthesis of [Pt(ppy)Cl(**L3**)], **[Pt-L3]**:* Platinum precursor **[Pt-0]** (160.9 mg, 298.15 µmol) and ligand **L3** (100 mg, 298.15 µmol) were dissolved in 10 mL of DMF and heated under reflux for 24 h. Then, the solvent was evaporated to dryness and the solid was washed with Et_2O (2 x 10 mL) under stirring and recrystallized in $CHCl_3$ in the freezer (5 mL), filtered and dried under vacuum. Pale yellow solid (128.3 mg, 60% yield). **^{1}H NMR (400 MHz, $CDCl_3$):** δ 9.81 (d, $J_{Pt\text{-}H}$ = 38.5, $J_{H\text{-}H}$ = 5.6 Hz, 1H; Ha), 9.41 (d, $J_{H\text{-}H}$ = 7.8 Hz, 1H; H1), 8.63 (d, $J_{H\text{-}H}$ = 4.8 Hz, 1H; H_{arom}), 8.35 (d, $J_{H\text{-}H}$ = 7.9 Hz, 1H; H4), 7.79 (m, 4H; Hc, Hd, H2, H_{arom}), 7.61 (m, 2H; 2 H_{arom}), 7.47 (m, 2H; 2 H_{arom}), 7.39 (m, 4H; Hh, 3 H_{arom}), 7.31(m, 3H; H3, 2 H_{arom}) 7.16 (t, $J_{H\text{-}H}$ = 6.7 Hz, 1H; Hb), 6.98 (t, $J_{H\text{-}H}$ = 7.5 Hz, 1H; Hg), 6.82 (d, $J_{H\text{-}H}$ = 7.5 Hz, 1H; Hf), 6.26 (d, $J_{Pt\text{-}H}$ = 41.3, $J_{H\text{-}H}$ = 7.6 Hz, 1H; He), 6.11 ppm (d, $J_{H\text{-}H}$ = 15.9 Hz, 1H, C*H*H), 5.98 ppm (d, $J_{H\text{-}H}$ = 15.9 Hz, 1H, CH*H*). **^{13}C{^{1}H} NMR (101 MHz, $CDCl_3$):** *δ* 151.2 (Ca), 150.4 (C_q), 148.8 (C4), 148.1 (C_q), 144.6 (C_q), 141.1 (C_q), 140.7 (C_q), 139.1 (C_q), 138.5 (CH_{arom}), 137.8 (C_q), 136.8 (CH_{arom}), 134.6 (C_q), 133.3 (CH), 133.1 (C_q), 131.6 (Ce), 130.1 (Cf), 129.0 (CH_{arom}), 128.3 (CH_{arom}), 128.0 (CH_{arom}), 127.8 (CH_{arom}), 126.60(CH_{arom}), 126.1 (CH_{arom}), 125.5 (CH_{arom}), 125.1 (CH_{arom}), 124.7 (CH_{arom}), 124.4 (CH_{arom}), 123.3 (CH_{arom}), 123.1 (Cg), 123.0 (CH_{arom}), 122.0 (CH_{arom}), 121.6 (Cb), 111.3 (CH_{arom}), 49.6 ppm (CH_2). Due to the low resolution of the ^{13}C{^{1}H} and the HSQC NMR experiments one Cq of ppy$^-$ approx. at 167 ppm has been lost and all the carbons could not be assigned. **FT-IR (ATR) selected bands** 1610-1584 ($\nu_{C=N,\ Py}$), 1471-1445 ($\nu_{C=N,\ imid}$), 523-503 ($\nu_{Pt\text{-}N}$) cm^{-1} **HR-MS (*m/z*):** [M-Cl]$^+$ calcd for $[C_{34}H_{25}N_4Pt]^+$, 684.172; found, 684.1746. **Elemental analysis**: calcd for $C_{34}H_{25}ClN_4Pt \cdot (H_2O)$ = C, 55.32; H, 3.69; N, 7.59; found C, 55.16; H, 3.83; N, 7.19.

*Synthesis of [Pt(ppy)Cl(**L4**)], **[Pt-L4]**:* Platinum precursor **[Pt-0]** (131.8 mg, 244.21 μmol) and ligand **L4** (100 mg, 244.21 μmol) were dissolved in 10 mL of DMF and heated at 65 ºC for 72 h. Then, the solvent was evaporated to dryness and the solid was washed with Et_2O (2 x 10 mL) under stirring and recrystallized in $CHCl_3$ in the freezer (5 mL), filtered and dried under vacuum. Pale yellow solid (74.3 mg, 38% yield). **^{1}H NMR (400 MHz, $CDCl_3$):** δ 9.83 (d, $J_{Pt\text{-}H}$ = 38.9, $J_{H\text{-}H}$ = 5.09 Hz, 1H; Ha), 9.47 (d, $J_{H\text{-}H}$ = 7.9 Hz, 1H; H1), 8.51 (d, $J_{H\text{-}H}$ = 4.8 Hz, 1H; H4), 8.40 (d, $J_{H\text{-}H}$ = 8.2 Hz, 1H; H_{arom}), 8.37 (d, $J_{H\text{-}H}$ = 9.2 Hz, 1H; H_{arom}), 8.24 (m, 3H; 3 H_{arom}), 8.05 (m, 4H; 4 H_{arom}), 7.83 (dt, $J_{H\text{-}H}$ = 7.7, 1.43 Hz, 1H; Hc), 7.74 (dt, $J_{H\text{-}H}$ = 7.8, 1.6 Hz, 1H; H2), 7.62 (d, $J_{H\text{-}H}$ = 8.3 Hz, 1H; Hd), 7.56 (d, $J_{H\text{-}H}$ = 8.02 Hz, 1H; H_{arom}), 7.35 (m, 3H; Hh, 2 H_{arom}), 7.20 (m, 3H; Hb, H3, H_{arom}), 7.00 (t, $J_{H\text{-}H}$ = 7.5 Hz,1H; Hg), 6.87 (t, J = 7.5 Hz, 1H; Hf), 6.72 (d, $J_{H\text{-}H}$ = 16.6 Hz, 1H; CH*H*), 6.66 (d, $J_{H\text{-}H}$ = 16.6 Hz, 1H; C*H*H), 6.36 (d, $J_{Pt\text{-}H}$ = 41.7, $J_{H\text{-}H}$ = 7.48 Hz, 1H; He). **^{13}C{^{1}H} NMR (101 MHz, $CDCl_3$):** δ 167.6 (C_q), 151.2 (Ca), 150.3 (C_q), 148.8 (C4), 148.1 (C_q), 144.5 (C_q), 141.1 (C_q), 140.6 (C_q), 138.5 (Cc), 136.8 (C2), 135.8 (C_q), 134.4 (C_q), 131.6 (Ce), 130.1 (Cf), 129.4 (2 CH_{arom}), 128.2 (CH_{arom}), 128.1 (C1), 127.1 (2 CH_{arom}), 125.5 (CH_{arom}), 125.1 (CH_{arom}), 124.4 (CH_{arom}), 123.3 (CH_{arom}), 123.1 (Cg), 121.9 (CH_{arom}), 121.5 (CH_{arom}), 118.1 (Cd), 111.3 (CH_{arom}), 48.6 ppm (CH_2). **FT-IR (ATR) selected bands** 1607-1584 ($\nu_{C=N}$, Py), 1483-1440 ($\nu_{C=N}$, imid), 488-450 ($\nu_{Pt\text{-}N}$) cm-1 **HR-MS (*m/z*)**: [M - Cl]$^+$ calcd for $[C_{40}H_{27}N_4Pt]^+$, 758.1883; found, 758.1876. **Elemental analysis**: calcd for $C_{40}H_{27}ClN_4Pt\cdot(H_2O)_{:}$ = C, 59.15; H, 3.60; N, 6.90; found C, 59.12; H, 3.80; N, 6.59.

X-ray crystallography: Data collection and refinement parameters for **[Pt-L2]**, **[Pt-L3]**, **[Pt-L4]** are summarized in Table SI1, SI3 and SI5 of the Supporting Information. A single crystal of the complexes was coated with high-vacuum grease, mounted on a glass fiber, and transferred to a Bruker SMART APEX CCD-based diffractometer equipped with a graphite-monochromated MoKa radiation source (λ=0.71073 a). The highly redundant datasets were integrated with SAINT[44] and corrected for Lorentzian and polarization effects. The absorption correction was based on the function fitting to the empirical transmission surface as sampled by multiple equivalent measurements with the program SADABS[45]. The software package WingX[46] was used for space-group determination, structure solution, and OLEX 2 1.2.10[47] was used for refinement by full-matrix least-squares methods based on F2. A successful solution by direct methods provided most non-hydrogen atoms from the E map. The remaining non-hydrogen atoms were located in an alternating series of least squares cycles and difference Fourier maps. All non-hydrogen atoms were refined with anisotropic displacement coefficients. Hydrogen atoms were placed by using a riding model and included in the refinement at calculated positions.

CCDC 1965455 (**[Pt-L2]**), 1965456 (**[Pt-L3]**), 1965457 (**[Pt-L4]**) contains the supplementary crystallographic data for this paper. These data are provided free of charge by The Cambridge Crystallographic Data Centre.

General Procedure of Stability and Binding to *d*GMP by NMR Spectroscopy. *Stability in DMF-d_7*: Complexes **[Pt-L1]-[Pt-L4]** were dissolved in 0.4 mL of DMF-d_7 (4 ·10^{-3} M), and ^{1}H NMR spectra were recorded during 24 h in a 400 MHz spectrometer. *Aquation Studies*: Over the previous solution, 100 μL of D_2O was added (5 ·10^{-3} M), and ^{1}H NMR spectra were recorded during 24 h in a 400 MHz spectrometer. *Addition of $AgNO_3$:* Over a solution coming from the stability in DMF-d_7/$D_2$0 (4:1) and after 24 in solution of the complexes, $AgNO_3$ was added and the ^{1}H NMR spectra were recorded after 24 h and 48h.

Binding Studies to dGMP: Over the previous solution, 5 mg of *d*GMP dissolved in 50 μL of D_2O was added, and ^{1}H NMR and ^{31}P spectra were recorded during 24 h in a 300 MHz spectrometer.

General Procedure of Stability by HRMS-ESI spectroscopy: Samples of the complexes **[Pt-L1]-[Pt-L4]** were prepared in DMF: NaCaC (2.5 mM, pH= 7, DMF 2%) in concentrations of 100 ppm. The sample was injected after 24 in solution in a 6545 Q-TOF (Agilent) (V_{inj}= 0.1 μL) Mobile phase: H_2O-formic acid:MeOH (30:70) (0.1 % of formic acid), flow 0.1 ml/min.

Biological activity. ***Antimicrobial activity***. The broth microdilution plate method according to CLSI criteria against ESKAPE (*Enteroccocus faecium, Staphylococcus aureus, Klebsiella pneumoniae, Acinetobacter baumannii, Pseudomonas aeruginosa*, and *Enterobacter cloacae*) pathogens.[48] The experiment involved 4 strains of pathogenic bacteria, *E. faecium* CECT 5253 (vancomycin resistant, Gram positive bacteria), *S. aureus* CECT 5190 (methicillin resistant, Gram positive bacteria), *A. baumannii* ATCC 17978 (Gram negative bacteria) and *P. aeruginosa* PAO1 (Gram negative bacteria). *A. baumannii, P. aeruginosa* and *S. aureus* strains were kept at 37 °C in Mueller-Hinton (MH) agar while *E. faecium* was maintained in Tryptic Soy (TS) agar at 37 °C. The Pt(II) complexes were dissolved in DMF and then diluted into nutrient liquid medium, Mueller Hinton Broth (MHB) up to a maximum of 2% of DMF content. Ampicillin was used a positive control. Serial dilutions of the compounds were prepared in MHB ranging from 100 μM to 3.1 μM (1:2 dilutions) in 96-well plates. Inoculated plates with a final concentration of 5×10^5 CFU/mL were incubated at 37 °C for 18-20h. Minimum Inhibitory concentration (MIC) was defined as the lowest concentration of tested drug that inhibited bacterial growth. The MICs reported are the mean values from at least three independent replicates. All tests were performed twice.

Cytotoxic activity. Approximately 1 × 10^4 for 24 h of treatment and 3 × 10^3 of SW480 cells for 72 h were cultured in 96-well plates in 200 μl culture medium per well (DMEM medium), supplemented with 10% newborn calf serum and 1% amphotericin-penicillin-streptomycin solution. Cells were incubated at 37 °C under a 5% CO_2 atmosphere during 24h and then treated with different concentrations of the tested drugs. The DMF content was kept equal or below 0.5% for 24 h of treatment and 0.2% for 72 h of treatment in order to avoid vehicle interferences. In these conditions, 100 μM is the highest tested concentration for all the compounds in case of 24h of treatment whereas for 72h of treatment is 25 μM for all the compounds except for **[L4]** and **[Pt-L4]** that could be tested at maximum 15 μM. After 24 h or 72 h of incubation, the treatment was retired and cells were incubated with 100 μl of MTT (3-(4,5-dimethyltiazol-2-yl)-2,5-diphenyltetrazoliumbromide) (Sigma Aldrich) dissolved in culture medium (500 μg/ml) for a further period of 3 h. At the end of the incubation, the formazan was dissolved by adding 100 μL of solubilizing solution (10 %SDS and 0.01M HCl) to each well. Then, plates were incubated at 37 °C with soft agitation. After 18 h, absorbance was read at 590 nm in a microplate reader (Cytation 5 Cell Imaging Multi-Mode Reader (Biotek Instruments, USA)). Four replicates per dose were included. The IC_{50} values, that is, the concentrations which produced 50% inhibition of cell viability, were calculated from MTT data using nonlinear regression of the GraphPadPrism Software Inc. (version 6.01) (USA). Cytotoxicity experiments under irradiation were carried out by irradiating 5 min the 96-well plates with UV light (λ = 365 nm, 20 mW/cm2) after 1 h of incubation with the complexes under study. Then, cells were incubated for another 23 and MTT was added following the procedure described above.

Cellular Uptake. SW480 cells were seeded at a density of 1.5 × 10^5 in 12-wells plates in 2 ml of culture medium per well. Cells were incubated at 37 °C under a 5% CO_2 atmosphere during 24h and then treated with 2μM of the tested drugs and incubated for a further period of 24h. Then, cells were washed twice with DPBS (Dulbecco's Phosphate Buffered Saline) and harvested. The

pellets were resuspended in 1 mL of DPBS. In each case, 10 µL were used to count cells. Then, cells were digested for ICP-MS with 65% HNO_3 during 24 h. Finally, solutions were analyzed in an 8900 Triple Quadrupole ICP-MS (Agilent Technologies). Data are reported as the mean ± the standard deviation (n = 3).

BSA Native gel electrophoresis. BSA is supplied as crystallized and lyophilized powder (Sigma-Aldrich). BSA working solutions were incubated overnight with different concentrations of the Pt-complexes at [complex]/ [protein] concentration ratios of 10 and 20 in sodium cacodylate buffer (NaCaC, 2.5 mM, pH=7) at 37 °C with agitation. Then, 6 µL of loading buffer (0.01% bromophenol blue and 20% glycerol in Tris HCl buffer (0.5 M, pH 6.8) and 6 µL of the sample solutions were loaded onto a 10 % polyacrylamide gel. Gels were run in native PAGE buffer (250 mM Tris Base, 1.92 M glycine, pH = 8.3) at 6.6 V/cm for 4 h at 4ºC to avoid thermal denaturation of the protein. Finally, gels were stained with Coomassie brilliant blue R-250 and visualized with a Gel Doc XR+ Imaging System (Bio Rad).

DNA binding ability. DNA binding of the Platinum(II) complexes was studied by agarose gel electrophoresis. Plasmid DNA (pUC18) was isolated from the strain DH5α of *Escherichia coli* with the use of Quiagen DNA purification kit. 20 µM in base pairs of pUC18 was incubated overnight at 37 °C with different concentrations of the Pt-complexes or cisplatin as positive control for DNA covalent binding. A vehicle control, pUC18 treated with 2% DMF was included. Samples were loaded onto a 1% agarose gel containing 0.05 µg/mL ethidium bromide. Electrophoresis was run at 5 V/cm for 1 h in TBE ×1 buffer, and the gel was visualized with a Gel Doc XR+ Imaging System (Bio-Rad). *Circular Dichroism measurements* were performed with Calf thymus DNA (Sigma-Aldrich) dissolved in water and sonicated to obtain short polynucleotide fragments (*ca*. 1000 base pairs). Solutions were prepared with doubly distilled water from a Puranity TU System with UV lamp and ultrafilter (VWR). To keep the pH constant at pH = 7.0, solutions were prepared using 2.5 mM of sodium cacodylate (NaCaC) as buffer. Several solutions at [DNA]/[Pt complexes] = 1.0 were prepared and measured freshly and after 24h of incubation in a MOS-450 biological spectrophotometer (Bio-Logic SAS, Claix, France).

ASSOCIATED CONTENT

Supporting Information

Selected ^{1}NMR spectra and HR-MS spectrum, Crystallographic parameters and representation of spatial interactions, absorption spectra of the ligands, NMR spectra of stability in DMSO-d_6, DMF-d_7, D_2O, and after the addition of $AgNO_3$, and binding to *d*GMP; HR-MS spectra of stability of the Pt complexes in buffer: DMF; Absorption y emission spectra of the ligands L1-L4; cells visualization and MIC values of antimicrobial activity; electrophoresis of BSA and electrophoresis of the plasmid at different concentrations of cisplatin. The Supporting Information is available free of charge on the ACS Publications website.

AUTHOR INFORMATION

Corresponding Author

* M. Vaquero: mvaquero@ubu.es.
* B. García: begar@ubu.es.

Author Contributions

‡These authors contributed experimentally equally to the work.

Funding Sources

The authors gratefully acknowledge the financial support by La Caixa Foundation (LCF/PR/PR12/11070003), Consejería de Educación-Junta de Castilla y León-FEDER (BU042U16-BU305P18), Ministerio de Ciencia, Innovación y Universidades (RTI2018-102040-B-100). M.V. is grateful for the financial support received from the Consejería de Educación-Junta de Castilla y León-FEDER (BU042U16-BU305P18).

Notes

The authors declare no competing financial interests.

ACKNOWLEDGMENT

We are indebted to P. Castroviejo and M. Mansilla (PCT of the Universidad de Burgos) for technical support, and A. M. Rodríguez (Universidad de Castilla-La Mancha) for her advice in the crystallographic resolution.

REFERENCES

(1) Jia, P.; Ouyang, R.; Cao, P.; Tong, X.; Zhou, X.; Lei, T.; Zhao, Y.; Guo, N.; Chang, H.; Miao, Y.; Zhou, S. Recent Advances and Future Development of Metal Complexes as Anticancer Agents. *J. Coord. Chem.* **2017**, *70*, 2175–2201.

(2) Kelland, L. The Resurgence of Platinum-Based Cancer Chemotherapy. *Nat. Rev. Cancer* **2007**, *7*, 573–584.

(3) Johnstone, T. C.; Suntharalingam, K.; Lippard, S. J. The Next Generation of Platinum Drugs: Targeted Pt(II) Agents, Nanoparticle Delivery, and Pt(IV) Prodrugs. *Chem. Rev.* **2016**, *116*, 3436–3486.

(4) Rosenberg, B.; Van Camp, L.; Krigas, T. Inhibition of Cell Division in Escherichia Coli by Electrolysis Products from a Platinum Electrode. *Nature* **1965**, *205*, 698–699.

(5) Cai, L.; Yu, C.; Ba, L.; Liu, Q.; Qian, Y.; Yang, B.; Gao, C. Anticancer Platinum-Based Complexes with Non-Classical Structures. *Appl. Organomet. Chem.* **2018**, *32*, 1–17.

(6) Deo, K. M.; Ang, D. L.; McGhie, B.; Rajamanickam, A.; Dhiman, A.; Khoury, A.; Holland, J.; Bjelosevic, A.; Pages, B.; Gordon, C.; Aldrich-Wright, J. R. Platinum Coordination Compounds with Potent Anticancer Activity. *Coord. Chem. Rev.* **2017**, *375*, 148–163.

(7) Bai, L.; Gao, C.; Liu, Q.; Yu, C.; Zhang, Z.; Cai, L.; Yang, B.; Qian, Y.; Yang, J.; Liao, X. Research Progress in Modern Structure of Platinum Complexes. *Eur. J. Med. Chem.* **2017**, *140*, 349–382.

(8) Oun, R.; Moussa, Y. E.; Wheate, N. J. The Side Effects of Platinum-Based Chemotherapy Drugs: A Review for Chemists. *Dalton. Trans.* **2018**, *47*, 6645–6653.

(9) Cleare, M. J.; Hydes, P. C.; Malerbi, B. W.; Watkins, D. M. Anti-Tumour Platinum Complexes : Relationships between Chemical Properties and Activity. *Biochimie* **1978**, *60*, 835–850.

(10) Perez, R. P. Cellular and Molecular Determinants of Cisplatin Resistance. *Eur. J. Cancer* **1998**, *34*, 1535–1542.

(11) Kelland, L. R.; Sharp, S. Y.; O'Neill, C. F.; Raynaud, F. I.; Beale, P. J.; Judson, I. R. Discovery and Development of Platinum Complexes Designed to Circumvent Cisplatin Resistance. *J. Inorg. Biochem.* **1999**, *77*, 111–115.

(12) Maji, M.; Karmakar, S.; Ruturaj; Gupta, A.; Mukherjee, A. Oxamusplatin: A Cytotoxic Pt(Ii) Complex of a Nitrogen Mustard with Resistance to Thiol Based Sequestration Displays Enhanced Selectivity towards Cancer. *Dalton Trans.*, **2020**, *49*, 2547-2558

(13) Chen, H. H. W.; Kuo, M. T. Role of Glutathione in the Regulation of Cisplatin Resistance in Cancer Chemotherapy. *Met. Based. Drugs* **2010**, *2010*, 430939.

(14) Mock, C.; Puscasu, I.; Rauterkus, M. J.; Tallen, G.; Wolff, J. E. A.;

Krebs, B. Novel Pt(II) Anticancer Agents and Their Pd(II) Analogues: Syntheses, Crystal Structures, Reactions with Nucleobases and Cytotoxicities. *Inorganica Chim. Acta* **2001**, *319*, 109–116.

(15) Gumus, F.; Pamuk, I.; Ozden, T.; Yildiz, S.; Diril, N.; Oksuzoglu, E.; Gur, S.; Ozkul, A. Synthesis, Characterization and in Vitro Cytotoxic, Mutagenic and Antimicrobial Activity of Platinum(II) Complexes with Substituted Benzimidazole Ligands. *J. Inorg. Biochem.* **2003**, *94*, 255–262.

(16) Casas, J. S.; Castiñeiras, A.; García-Martínez, E.; Parajó, Y.; Pérez-Parallé, M. L.; Sánchez-González, A.; Sordo, J. Synthesis and Cytotoxicity of 2-(2′-Pyridyl)Benzimidazole Complexes of Palladium(II) and Platinum(II). *Zeitschrift fur Anorg. und Allg. Chemie* **2005**, *631*, 2258–2264.

(17) Zhao, J.; Zhao, D.; Zhao, Y.; Shu, H.; Hu, J. Photoluminescence and in Vitro Cytotoxicity of Benzimidazole-Based CuI/PtII Complexes. *Polyhedron* **2016**, *119*, 7–13.

(18) Serratrice, M.; Maiore, L.; Zucca, A.; Stoccoro, S.; Landini, I.; Mini, E.; Massai, L.; Ferraro, G.; Merlino, A.; Messori, L.; Cinellu, M. A. Cytotoxic Properties of a New Organometallic Platinum(II) Complex and Its Gold(I) Heterobimetallic Derivatives. *Dalton. Trans.* **2016**, *45*, 579–590.

(19) Pérez-Arnaiz, C.; Leal, J.; Busto, N.; Carrión, M. C.; Rubio, A. R.; Ortiz, I.; Barone, G.; Díaz De Greñu, B.; Santolaya, J.; Leal, J. M.; Vaquero, M.; Jalón, F. A; Manzano, B. R.; García, B. Role of Seroalbumin in the Cytotoxicity of Cis-Dichloro Pt(II) Complexes with (N^N)-Donor Ligands Bearing Functionalized Tails. *Inorg. Chem.* **2018**, *57*, 6124–6134.

(20) Mansour, A. M.; Shehab, O. R. Lysozyme and DNA Binding Affinity of Pd(II) and Pt(II) Complexes Bearing Charged N,N-Pyridylbenzimidazole Bidentate Ligands. *Dalton. Trans.* **2018**, 3459–3468.

(21) Gumus, F.; Pamuk, I.; Ozden, T.; Yildiz, S.; Diril, N.; Oksuzoglu, E.; Gur, S.; Ozkul, A. Synthesis, Characterization and in Vitro Cytotoxic, Mutagenic and Antimicrobial Activity of Platinum(II) Complexes with Substituted Benzimidazole Ligands. *J. Inorg. Biochem.* **2003**, *94*, 255–262.

(22) Florio, D.; Iacobucci, I.; Ferraro, G.; Mansour, A.M.; Morelli, G.; Monti, M.; Merlino, A.; Marasco, D. Role of the Metal Center in the Modulation of the Aggregation Process of Amyloid Model Systems by Square Planar Complexes Bearing 2-(2'-Pyridyl)Benzimidazole Ligands. *Pharmaceuticals* **2019**, *12*, 154.

(23) Mitra, K.; Gautam, S.; Kondaiah, P.; Chakravarty, A. R. BODIPY-Appended 2-(2-Pyridyl)Benzimidazole Platinum(II) Catecholates for Mitochondria-Targeted Photocytotoxicity. *ChemMedChem* **2016**, *11*, 1956–1967.

(24) Huang, W.-K.; Cheng, C.-W.; Chang, S.-M.; Lee, Y.-P.; Diau, E. W.-G. Synthesis and Electron-Transfer Properties of Benzimidazole-Functionalized Ruthenium Complexes for Highly Efficient Dye-Sensitized Solar Cells. *Chem. Commun.* **2010**, *46*, 8992–8994.

(25) Niedermair, F.; Waich, K.; Kappaun, S.; Mayr, T.; Trimmel, G.; Mereiter, K.; Slugovc, C. Heteroleptic K2(N,C2)-2-Phenylpyridine Platinum Complexes: The Use of Bis(Pyrazolyl)Borates as Ancillary Ligands. *Inorganica Chim. Acta* **2007**, *360*, 2767–2777.

(26) Okada, T.; El-Mehasseb, I. M.; Kodaka, M.; Tomohiro, T.; Okamoto, K.; Okuno, H. Mononuclear Platinum(II) Complex with 2-Phenylpyridine Ligands Showing High Cytotoxicity against Mouse Sarcoma 180 Cells Acquiring High Cisplatin Resistance. *J. Med. Chem.* **2001**, *44*, 4661–4667.

(27) Esmaeilbeig, A.; Samouei, H.; Abedanzadeh, S.; Amirghofran, Z. Synthesis, Characterization and Antitumor Activity Study of Some Cyclometalated Organoplatinum(II) Complexes Containing Aromatic N-Donor Ligands. *J. Organomet. Chem.* **2011**, *696*, 3135–3142.

(28) Sommerfeld, N. S.; Gülzow, J.; Roller, A.; Cseh, K.; Jakupec, M. A.; Grohmann, A.; Galanski, M.; Keppler, B. K. Antiproliferative Copper(II) and Platinum(II) Complexes with Bidentate N,N-Donor Ligands. *Eur. J. Inorg. Chem.* **2017**, 3115–3124.

(29) Křikavová, R.; Hanousková, L.; Dvořák, Z.; Trávníček, Z. Dichlorido-Platinum(II) Complexes with Kinetin Derivatives as Promising Cytotoxic Agents Avoiding Resistance of Cancer Cells: Contrasting Results between Cisplatin and Oxaliplatin Analogues. *Polyhedron* **2015**, *90*, 7–17.

(30) Omary, M. A.; Patterson, H. H. Luminescence, Theory. *Encycl. Spectrosc. Spectrom. (Second Ed.* **1999**, 372–1391.

(31) Jenkins, D. M.; Senn, J. F.; Bernhard, S. Cyclometalated Platinum(Ii) Diimine Complexes: Synthetically Tuning the Photophysical and Electrochemical Properties. *Dalton. Trans.* **2012**, *41*, 8077–8085.

(32) Casini, A.; Reedijk, J. Interactions of Anticancer Pt Compounds with Proteins: An Overlooked Topic in Medicinal Inorganic Chemistry? *Chem. Sci.* **2012**, *3*, 3135–3144.

(33) Kragh-Hansen, U. Molecular Aspects of Ligand Binding to Serum Albumin. *Pharmacol. Rev.* **1981**, *33*, 17–53.

(34) Reily, M. D.; Marzilli, L. G. Novel, Definitive NMR Evidence for N(7), .Alpha.PO4 Chelation of 6-Oxopurine Nucleotide Monophosphates to Platinum Anticancer Drugs. *J. Am. Chem. Soc.* **1986**, *108*, 8299–8300.

(35) Kozelka, J.; Barre, G. The Phosphodiester Groups of d(TpT)– and d(TpG)- Coordinate to Platinum(II) in N,N-Dimethylformamide. *Chem. – A Eur. J.* **2006**, *3*, 1405–1409.

(36) Keck, M. V; Lippard, S. J. Unwinding of Supercoiled DNA by Platinum-Ethidium and Related Complexes. *J. Am. Chem. Soc.* **1992**, *114*, 3386–3390.

(37) A. D. Bates and A. Maxwell , DNA Topology , Oxford University Press, 2005

(38) Pérez-Arnaiz, C.; Busto, N.; Leal, J. M.; García, B. New Insights into the Mechanism of the DNA/Doxorubicin Interaction. *J. Phys. Chem. B* **2014**, *118*, 1288–1295.

(39) Brana, M. F.; Cacho, M.; Gradillas, A.; de Pascual-Teresa, B.; Ramos, A. Intercalators as Anticancer Drugs. *Curr. Pharm. Des.* **2005**, *7*, 1775–1780.

(40) Qiu, K.; Chen, Y.; Rees, T. W.; Ji, L.; Chao, H. Organelle-Targeting Metal Complexes: From Molecular Design to Bio-Applications. *Coord. Chem. Rev.* **2019**, *378*, 66–86.

(41) Jungwirth, U.; Kowol, C. R.; Keppler, B. K.; Hartinger, C. G.; Berger, W.; Heffeter, P. Anticancer Activity of Metal Complexes: Involvement of Redox Processes. *Antioxidants Redox Signal.* **2011**, *15*, 1085–1127.

(42) Dasari, S.; Bernard Tchounwou, P. Cisplatin in Cancer Therapy: Molecular Mechanisms of Action. *Eur. J. Pharmacol.* **2014**, *740*, 364–378.

(43) Shavaleev, N. M.; Bell, Z. R.; Easun, T. L.; Rutkaite, R.; Ward, M. D. Complexes of Substituted Derivatives of 2-(2-Pyridyl)Benzimidazole with Re(I), Ru(II) and Pt(II): Structures, Redox and Luminescence Properties. *Daltonon Trans.* **2004**, 3678–3688.

(44) No Title. *B. N. Axs, SAINT Area-Detector Integr. Program. SAINT+ v7.12a.; Madison, Wisconsin, USA 2004.*

(45) No Title. *G. M. Sheldrick, SADABS A Progr. Empir. Absorpt. Correct. Version 2004/ 1, Univ. Gçttingen, Gçttingen, Ger. 2004.*

(46) Farrugia, L. J.; IUCr. WinGX and ORTEP for Windows : An Update. *J. Appl. Crystallogr.* **2012**, *45*, 849–854.

(47) Dolomanov, O. V.; Bourhis, L. J.; Gildea, R. J.; Howard, J. A. K.; Puschmann, H. OLEX2: A Complete Structure Solution, Refinement and Analysis Program. *J. Appl. Crystallogr.* **2009**, *42*, 339–341.

(48) Clinical and Laboratory Standards Institute. Performance standards for antimicrobial susceptibility testing: 17th informational supplement M07-A9. Clinical and Laboratory Standards Institute, Wayne, PA. 2012.

SYNOPSIS TOC: Cytotoxicity and binding mode of the cyclometalated platinum(II) complexes are determined by the bulkiness of the appended aromatic substituents in the 2(2-Pyridil)benzimidazole scaffold. Complexes with small groups are able to bind covalently to DNA and present two-fold more cytotoxicity than cisplatin, while the complexes with bulky condensed aromatic rings are able to intercalate into DNA and are non-cytotoxic.